Sensor Array for Evaluation of Gait Cycle

Slavomir KARDOS, Stanislav SLOSARCIK, Peter BALOG

Department of Technologies in Electronics, Faculty of Electrical Engineering and Informatics, Technical University of Kosice, Letna 9, 042 00 Kosice, Slovak Republic

slavomir.kardos@tuke.sk, stanislav.slosarcik@tuke.sk, peter.balog.2@tuke.sk

DOI: 10.15598/aeee.v17i4.3352

Abstract. *The gait motion is an essential part of the life of every human being. The evaluation of human motion is a subject of complex approach and knowledge in the biomechanics area with application in orthopedics, therapy and commercial sporting applications. The monitoring and diagnostics allow determining the background of motion individualities and the defects reasons and impacts. The article describes the possibilities of gait cycle sensing, which has the potential for use in medical diagnostics and rehabilitation process monitoring. The system incorporates a matrix of four FSR (Force Sensing Resistor) pressure sensors and an accelerometric unit for the possibility of posture and step cycle evaluation so that it can be utilizable at diagnostic or rehabilitation during gait cycle re-training or sporting activities monitoring.*

Keywords

Accelerometer, FSR sensor, gait sensing, human motion, microcontroller, sensor array.

1. Introduction

Real-time or logged sensing of gait parameters allows the human gait analysis in medical praxis, which has a wide application area in the rehabilitation process and accordingly allows early discovering of some degradation processes. For the purpose of the gait cycle monitoring, the force and inertial sensors are mainly used. The following analysis is applied using known reference data of normal and defective profiles of gait [1], [2] and [3].

The sensors for movement, force, loading or pressure measurement are produced in various constructions. According to the application and required sensitivity of sensing, the concrete ones are used [4], [5] and [6]. In technical as well as medical praxis, the FSRs are widely applied for measurement of pressure or loading related parameters. They consist of a layer of a conductive polymer, which change its nominal resistance by application of the force at the surface of the sensor active area. The inner structure incorporates a system of electrically conductive composition with the non-conductive particles suspended in the solid polymer matrix. The size of the active particles is in sub-micrometer order, and they are further composed to compensate for the resistivity temperature dependence. The application of the perpendicular force at the surface of the FSR sensor causes the dilatation of the structure and consequently, the resistance decreasing as well. The meaningful benefit of these sensors is in the thin profile of less than 0.5 mm in thickness [7].

Utilization of accelerometric units allows high sensitive inertial measurements of motion parameters, which has the impact into a wide range of industrial applications. According to the particular type, they have comparatively low production costs and good mechanical resistance. Moreover, they are the only alternative in many applications due to the size and sensitivity.

2. Sensor System with Utilization of FSR and Accelerometer

The human posture and gait are given by the individual givenness and habits that are influenced by a kind of life as well as degeneration processes. The human sole is an area of naturally uneven distributed loading during the gait cycle. The distribution of the sole loading leads to sense it by a multi-channel sensor system with appropriate distributed sensor segments in the arrangement which allow the analysis of the gait. With regard to the character of the problematics, the four-channel loading sensor system was designed as an optimal setup which corresponds to the measurement in four sole areas (see Fig. 1). The first two measurement points were determined in the heel foot area, and the next two points are localized in front of the plantar arch area. Such application types require the implementation of the sensor matrix in the insole, including the requirements for the compact and thin profile according to its specific localization, resistance to the pressure and shear related mechanic stress and to the presence of the moisture in a full relative humidity range due to aggressive sweat influence possibility.

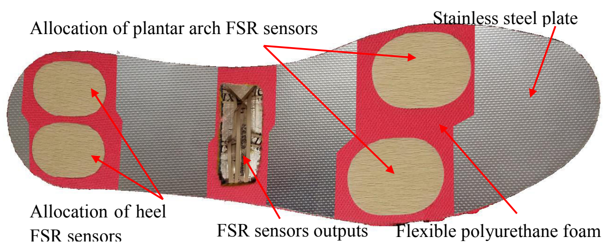

Fig. 1: Allocation of the FSR sensor array embedded in the insole.

Assuming the mentioned requirements, the Tekscan FlexiForce A201 force sensors (see Fig. 2) were applied as the sensing elements at the sensing points.

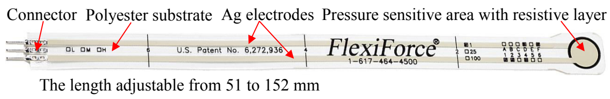

(a)

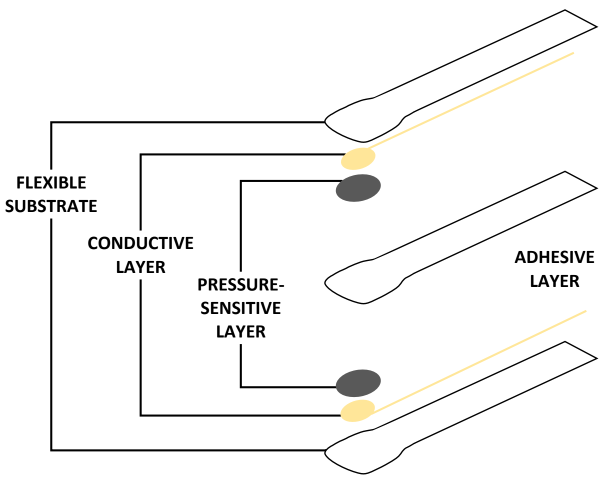

(b)

Fig. 2: The Tekscan FlexiForce A201 mechanical force / loading sensor (a) and the simplified structure of the sensor in decomposed view (b) [7].

The sensor element is 0.2 mm thin, flexible component, which is easy to integrate into target applications which have the space limitations. The overall sensor width is 14 mm, and the diameter of the active area is 9.53 mm. The construction of the sensor incorporates two flexible polyester substrates on which the conductive silver interconnection layer is applied. The mechanical stress-sensitive layer is applied between the substrates, and the overall structure is laminated using polymer adhesive. The active sensing area is defined by circular silver layer electrodes, which are elongated through the flexible interconnection cable to the connector, where the length can be adjusted. The operational temperature range of the sensor is defined from -40 to 60 °C. The signal response time is guaranteed less than 5 µs, which is fully sufficient for the application [7] due to gait frequency and dynamics.

The sensing area of the pressure sensor is not sufficient enough for the distributed load sensing in the sense of the surface area so the additional mechanical elements were added in the form of the mechanical transducer and loading actuator. The mechanical transducer allows expanding the loading area of the outer part of the insole and the loading actuator allows the concentration of the loading to the sensing area (see Fig. 3). The four mechanical transducers were realized using molded polyamide. The incorporated loading actuators are disc-like profile elements with a round base, which are about 70 % of sensing area of the pressure sensor according to producer recommendations in the production data list. The loading force application has incorporated a shear force component which can cause the displacement of the disc element out of the sensing area. For the purpose of elimination of that unfavorable effect, the PET foil is inserted between the mechanical transducer element and disc actuator. In such a configuration, the protective foil will shift if shear force is present. So the disc element retains fixed to the pressure sensor. The mentioned sensor system arrangement is inserted between the two stainless-steel plates. The polyurethane foam was used as the filling medium to the rest of the system.

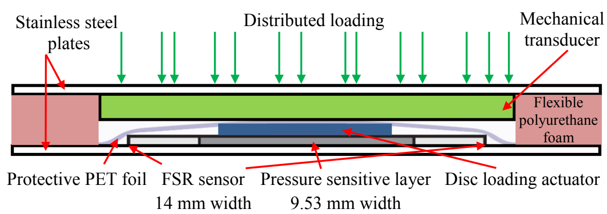

Fig. 3: The construction arrangement of an elemental sensing element with the mechanical transducer and the loading actuator.

The ADXL345 (Analog Devices) was utilized as the accelerometric unit for motion sensing, which provides preconditioned data in digital form (see Fig. 3). The accelerometer is based on variation of motion velocity sensing and in the orthogonal system, the 3-axis interpretation is needed [8]. In case of wide utilized capacitive MEMS (Micro-Electro-Mechanical-System) accelerometric system, the actual acceleration is proportional to the capacitance change and after conversion to the voltage change by:

$$a = \frac{kd}{mU} U_0 \quad (\mathrm{m \cdot s^{-2}}), \tag{1}$$

where k is the spring constant (stiffness of polycrystalline silicon spring), d is the idle-state gap between the electrodes in (m), and m in (kg) is related to a mass of the polycrystalline silicon seismic element.

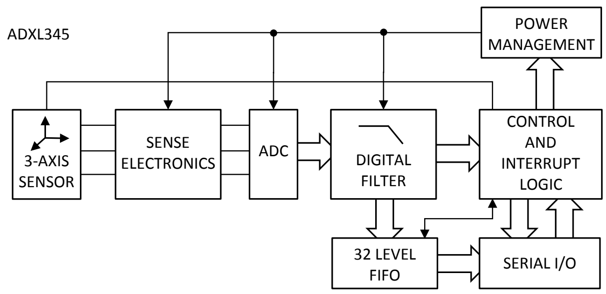

Fig. 4: The ADXL345 3-axis accelerometer unit with the signal preconditioning and I2C digital driver [8].

The accelerometer data are information about actual acceleration in $(\mathrm{m \cdot s^{-2}})$ so that it is possible to evaluate the dynamic variation of velocity in time under the given bandwidth. Individual accelerometer changes its measurement sensitivity (the change in output by the corresponding change in input) due to sinusoidal dependence. It means that the gravity produces the acceleration output proportional to the sine of the angle between the sensor (at the equipment) and the natural horizon (orthogonal to the gravity vector):

$$a_{(g)} = g \sin\theta \quad (\mathrm{m \cdot s^{-2}}), \tag{2}$$

where g is the gravitational or static acceleration in $(\mathrm{m \cdot s^{-2}})$, and θ is the inclination angle in (rad) relative to the horizon, so that its value is proportional to the inverse sine function of the of their ratio:

$$\theta = \sin^{-1} \frac{a_{(g)}}{g} \quad (\mathrm{rad}). \tag{3}$$

Consequently, the angle change during accelerometer data interpretation can be calculated by the triangle cosine theorem:

$$\phi = \cos^{-1} \frac{a_x b_x + a_y b_y + a_z b_z}{\sqrt{a_x^2 + a_y^2 + a_z^2}\sqrt{b_x^2 + b_y^2 + b_z^2}} \quad (\mathrm{rad}), \tag{4}$$

where a and b in $(\mathrm{m \cdot s^{-2}})$ are the acceleration values between the two accelerometer readings in the respective directions [9], [10] and [11].

3. The FSR and Accelerometer Signal Processing

The sensor system is followed by the electronic circuit, including four-channel FSR sensor signal preconditioning, microcontroller for data acquisition and preprocessing, power management including charging and wireless module for data transmission. Preconditioning of the signal from FSR sensors is realized by MCP6004 integrated quadruple analog operational amplifier (see Fig. 5(a)). The pressure sensing range and the sensitivity are adjustable by the reference and feedback of the amplifier.

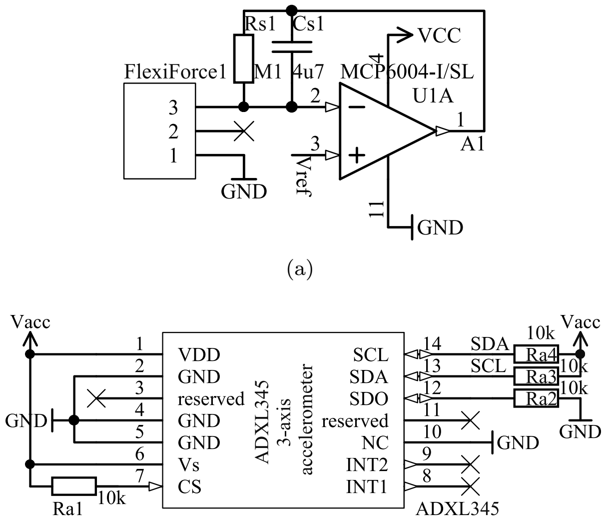

(a)

(b)

Fig. 5: The FSR sensors signal preconditioning amplifier circuitry (a) and the accelerometer sensor interfacing circuitry (b).

The single-source operation is more suitable for the portable application, moreover, without the meaningful linearity drop-out, but the feedback range is more limited than with the dual (symmetric) source. So that the signal conditioning of such type was used with the output voltage delimited by:

$$V_{out} = V_{ref} \frac{R_{FB}}{R_{FF}} \quad (\mathrm{V}), \tag{5}$$

where V_{ref} is the reference voltage in (V), R_{FB} is the feedback resistor resistance in (Ω) (R_s in the schematics on the Fig. 5), and R_{FF} is the sensor resistance in (Ω) (FlexiForce connector in Fig. 5).

The signal from the ADXL345 is conditioned by referencing at the reference conditions by the software. Also, the measurement range of the accelerometer is adjustable by software and is sufficient as ±2 g for standard gait. Due to I2C type digital bus, only the 10 kΩ pull-up resistors were added to the SDA and SCL communication pins (see Fig. 5(b)).

The digitalization of the signal from the FSR sensors is realized by the 10-bit ADC of Atmel ATmega328 microcontroller [12]. The pre-processed data are directed to SPP-C type Bluetooth 2.0 unit, which allows the communication with the microcontroller through standard UART serial bus. The power management of the microcontroller module includes the MCP73831T integrated charger driver, the miniature prismatic 130 mAh accumulator and the 10A45 5 V Switched-Mode Power Source (SMPS) boost converter [13], [14] and [15]. The overall electronic system functional block schematic diagram is described in Fig. 6 and the realized module in Fig. 7 with the description of the main components.

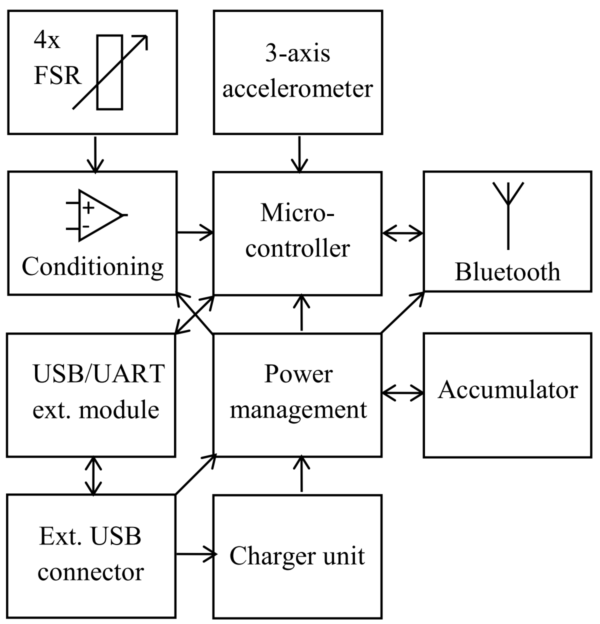

Fig. 6: The block diagram of the FSR and accelerometric sensor system with signal processing circuitry and microcontroller module components.

The accumulator energy capacity was calculated regarding the energetic needs of the overall system. Due to various components, the voltage levels also had to be adapted. The operational current consumption of the four FSR sensors is 0.4 mA including conditioning operational amplifier, and is limited by the current noise and interference level. The microcontroller current consumption is 9 mA, the Bluetooth unit consumes 8 mA during communication so that the power consumption of the overall system with additional loses at 5 V charge pump boost switching source is 100 mW in maximum. That results in approximately 5–6 hours of 130 mAh accumulator operation with the electronically limited voltage.

The prismatic Li-ion accumulator was selected due to its very low profile which with the surface mounted devices at the fiber-glass epoxy substrate results into only 3 mm overall thickness and 48 × 55 mm size of the module. This property perspectively allows the integration of the module into shoe insole together with the FSR sensors.

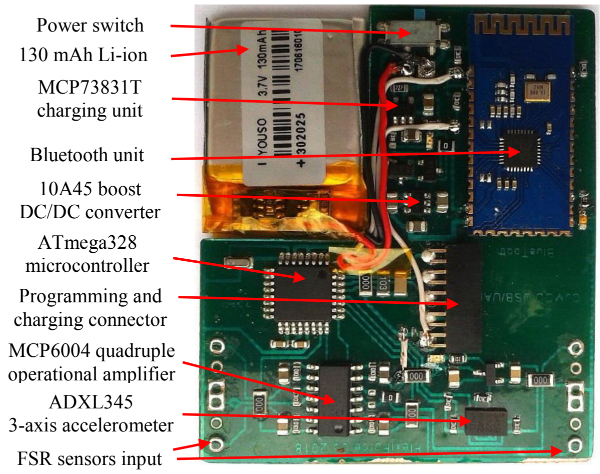

Fig. 7: The FSR and accelerometric sensor system signal processing microcontroller module including power management.

The microcontroller code provides initialization of sensor channels, setting of communication protocols and transfer rates for the digital buses, the data acquisition, its processing and consequent wireless transfer through the SPP-C Bluetooth unit to the PC application.

An FSR sensor application is preceded by initialization using the methodology stated in the product datasheet. The process started by loading of each sensor by 110 % of the operational range during 3 seconds and repeated five times. The next step included progressive loading by 1/3, 2/3 to the full loading. The initialization was not applied on a bare sensor, but the full mechanical chain described in Fig. 3 with resultant conversion curves in Fig. 8 was evaluated.

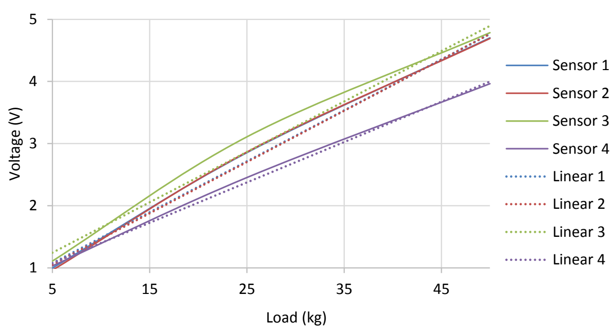

Fig. 8: The graphical dependencies of FSR sensors outputs which were conditioned by a recommended mechanical loading.

After the conditioning, measurement range and sensitivity setting, the sensor segments were evaluated for hysteresis in the loading range from 5 to 50 kg due to mechanical transducer and loading actuator influence. The resultant hysteresis (see Fig. 8) means up to 2 % deviation between increasing and decreasing loading at the particular sensor segment.

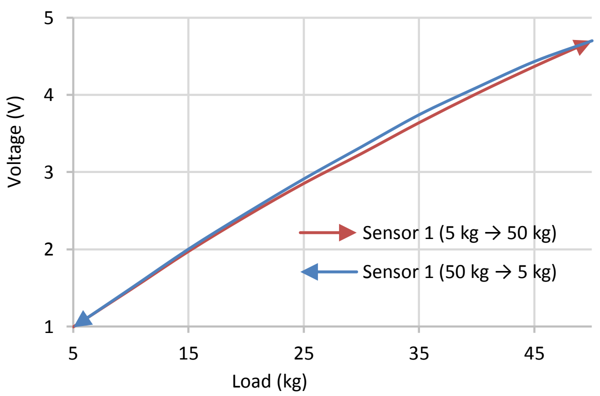

(a) Sensor 1.

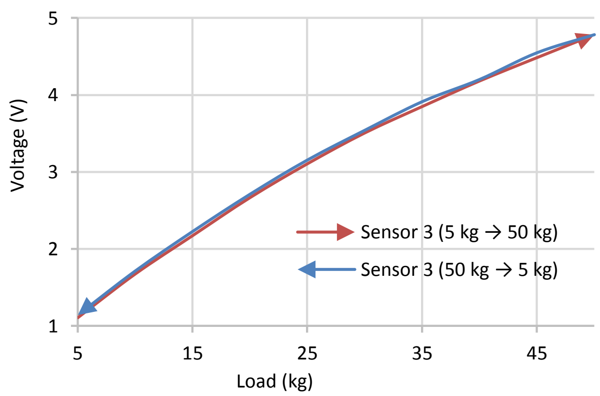

(b) Sensor 3.

Fig. 9: Graphical dependencies of conditioned FSR sensor hysteresis (the Sensor 1 from heel foot area and the Sensor 3 from the plantar arch area).

The experimental mechanical loading testing was realized at Testometric M250-2.5CT equipment. The resultant conversion characteristics of the sensor matrix were used for evaluation of loading interpretation, which is influenced by overall mechanical structure.

4. Interpretation Software

The FSR sensors data are helpful for posture as well as gait cycle loading analysis. In the module, the sensors are distributed according to relevant loading points in the plantar area so that the substantial differences between the left and right foot as well as deviations in comparison with a normal gait can be identified and analyzed. For the loading activity monitoring, the data acquisition with the graphical user interface (see Fig. 10) under the LabVIEW application was created with the further possibility of statistical treatment.

The post-processing of acquired data is realized in the Motion Logger application under the LabVIEW system [16], which was developed for the purposes of inertial sensors data processing.

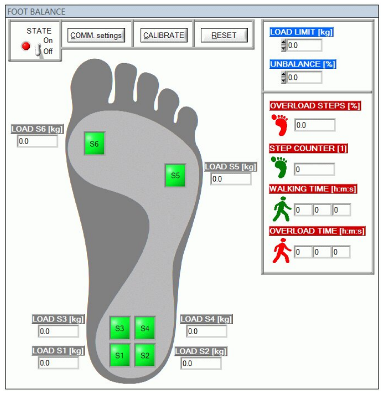

Fig. 10: The Foot Balance application graphical user interface in the LabVIEW system [15] for foot loading evaluation during a gait cycle.

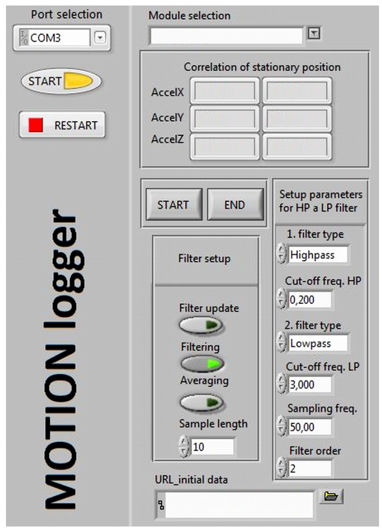

Fig. 11: The Motion Logger graphical user interface in the LabVIEW application for measurement of motion dynamics by the 3-axis accelerometer during a gait cycle.

The conditioning includes digital filtration realized by configurable bandpass Butterworth type filter [17], [18], [19], [20] and [21]. The purpose of the filter is to eliminate the static acceleration (gravity) components as well as the elimination of higher frequency components which occur by noise and signals generated by human body biological processes and other outer influences. In the LabVIEW application, there is a possibility to select the measurement mode and additional parameters including type and parameters of the filtration.

The additional parameters and functions are available as the offset, sample rate and averaging of data (see Fig. 11).

In Fig. 12 and Fig. 13, the experimental plots represent the single step signal for 2 selected channel FSR and 3-axis accelerometer output.

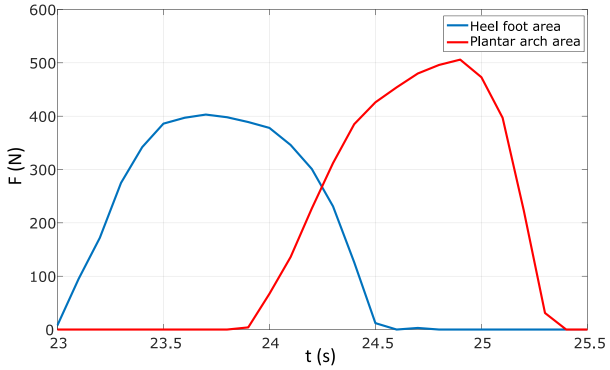

Fig. 12: The single step sample signal for the 2-channel FSR (for the heel foot area in blue and for the plantar arch area in red).

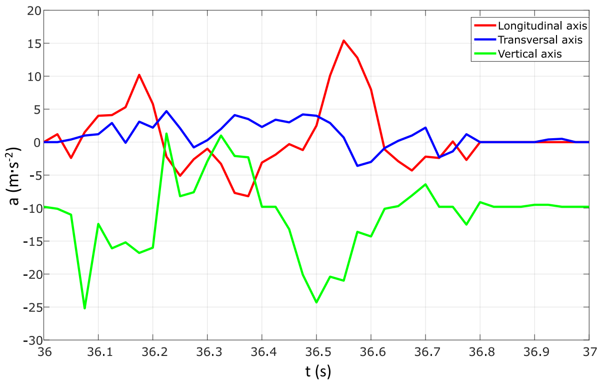

Fig. 13: The single step sample signal for the 3-axis accelerometer (for transversal axis in blue, for longitudinal axis in red and for vertical axis in green (unfiltered g)).

Based on FSR sensors and accelerometer data interpretation, the various types of posture and gait fault variations due to various factors can be recognized by the medical staff:

- uneven posture relative problems,
- progressing osteoporosis,
- muscular dystrophy,
- various gait irregularities.

The regeneration processes after the injury accidents can also be evaluated by comparison measurements. In addition, sports activities in amateur or professional scale can be evaluated using gait monitoring as well.

5. Conclusion

In the article, the four-channel loading and 3-axis motion sensor system with signal processing electronics module was designed and realized by the application requirements. The built sensor system consists of four FSR pressure sensors which were embedded in the heel and plantar arch area according to the physiology of the human foot, and the 3-axis accelerometer was attached to the processing electronics module. The microcontroller module includes the conditioning, digitalization, pre-processing and wireless transmission with the integrated accumulator and power management. The module was designed as a flat 3 mm structure which is applicable for embedding into a customized shoe insole. The system can be utilized for lower limb gait and loading analysis what means the active sensing of motion activities including rehabilitation drive simulator and for other sports and rehabilitation purposes. The continuing work is aimed to signal filtration and detailed interpretation of the accelerometer data.

Acknowledgment

This contribution is as a part of the work under the VEGA 1/0224/18 project. Special thanks belong to Martin Stupak for active participation on the work.

References

[1] DUNGL, P. *Ortopedie*. 1st ed. Praha: Grada, 2005. ISBN 80-247-0550-8.

[2] NECKEL, N., W. WISMAN and J. HIDLER. Limb Alignment and Kinematics Inside a Lokomat Robotic Orthosis. In: *International Conference of the IEEE Engineering in Medicine and Biology Society*. New York: IEEE, 2006, pp. 2698–2701. ISBN 1-4244-0032-5. DOI: 10.1109/IEMBS.2006.259970.

[3] VAREKA, I. and R. VAREKOVA. *Kineziologie nohy*. 1st ed. Olomouc: Univerzita Palackeho v Olomouci, 2009. ISBN 978-80-244-2432-3.

[4] KIRTLEY, C. *Intelligent sneaker insole*. United States Patent Application 20030009308, 2003.

[5] KIRTLEY, C. *Instrumented insole*. United States Patent Application 20030009308, 2003.

[6] HASELHURST, R. S. and J. R. CHRISTIANSEN. *System incorporating an insole pressure sensor and personal annunciator for use in gait assistive therapy*. United States Patent 7191644, 2007.

[7] Flexiforce Force Sensor Design & Integration Guide. In: *Tekscan* [online]. 2019. Available at: `https://www.tekscan.com`.

[8] ADXL345 ±16 g Digital Accelerometer, datasheet. In: *Analog Devices* [online]. 2019. Available at: www.analog.com.

[9] KAVANAGH, J. J. and H. B. MENZ. Accelerometry: A technique for quantifying movement patterns during walking. *Gait & Posture*. 2008, vol. 28, iss. 1, pp. 1–15. ISSN 0966-6362. DOI: 10.1016/j.gaitpost.2007.10.010.

[10] SHIN, J., D. SHIN, D. SHIN, S. HERSOO, H. KIM and M. LEE. Human Movement Detection Algorithm Using 3-Axis Accelerometer Sensor Based on Low-Power Management Scheme for Mobile Health Care System. In: *Advances in Grid and Pervasive Computing*. Heidelberg: Springer, 2010, pp. 81–90. ISBN 978-3-642-13067-0. DOI: 10.1007/978-3-642-13067-0_12.

[11] PEDLEY, M. Tilt Sensing Using a Three-Axis Accelerometer. In: *NXP* [online]. 2013. Available at: https://cache.freescale.com/files/sensors/doc/app_note/AN3461.pdf.

[12] ATmega328P 8-bit microcontroller, MCU/MCP datasheet. In: *Microchip* [online]. Available at: http://ww1.microchip.com/downloads/en/DeviceDoc/Atmel-7810-Automotive-Microcontrollers-ATmega328P_Datasheet.pdf.

[13] LESO, M., J. ZILKOVA, M. BIROS and P. TALIAN. SURVEY OF CONTROL METHODS FOR DC-DC CONVERTERS. *Acta Electrotechnica et Informatica*. 2018, vol. 18, iss. 3, pp. 41–46. ISSN 1335-8243. DOI: 10.15546/aeei-2018-0024.

[14] PAPEZ, V., D. BUSEK and J. PODZEMSKY. Radio-frequency solder film surface resistance measurement. In: *IEEE International Conference on Applied Electronics*. Pilsen: IEEE, 2011, pp. 1–4. ISBN 978-80-7043-930-2.

[15] AMARAL, A. and A. CARDOSO. VOLTAGE DOUBLER FOR AC-DC STEP-UP LINEAR POWER SUPPLIES: DESIGN, MODELLING AND SIMULATION. *Acta Electrotechnica et Informatica*. 2016, vol. 16, iss. 4, pp. 3–10. ISSN 1335-8243. DOI: 10.15546/aeei-2016-0025.

[16] LabVIEW System Design Software. In: *National Instruments* [online]. 2016. Available at: http://www.ni.com/labview/.

[17] BOGERT, T. Practical guide to data smoothing and filtering. In: *ISB Web* [online]. 2006. Available at: https://isbweb.org/software/sigproc/bogert/filter.pdf.

[18] HYUN, G. M. and E. T. JEUNG. Complementary Filter Design for Angle Estimation using MEMS Accelerometer and Gyroscope. In: *Academia Edu* [online]. 2015. Available at: http://www.academia.edu/6261055/Complementary_Filter_Design_for_Angle_Estimation_using_MEMS_Accelerometer_and_Gyroscope.

[19] SABAT, W., D. KLEPACKI, K. KURYLO and K. KAMUDA. Analysis of propagation process of conductive electromagnetic disturbances in AC/DC low power converter. In: *21st European Microelectronics and Packaging Conference (EMPC) & Exhibition*. Warsaw: IEEE, 2017, pp. 1–5. ISBN 978-0-9568086-4-6. DOI: 10.23919/EMPC.2017.8346920.

[20] MIHALOV, J., E. PIETRIKOVA, A. BALAZ, B. MADOS and N. ADAM. Potential of Low Cost Motion Sensors Compared to Programming Environments. *IEEE Journal of Applied Sciences*. 2018, vol. 15, iss. 6, pp. 155–177. ISSN 1785-8860. DOI: 10.12700/APH.15.6.2018.6.9.

[21] SEEL, T., J. RAISCH and T. SCHAUER. IMU-Based Joint Angle Measurement for Gait Analysis. *Sensors*. 2014, vol. 14, iss. 4, pp. 6891–6909. ISSN 1424-8220. DOI: 10.3390/s140406891.

About Authors

Slavomir KARDOS defended his Ph.D. thesis in the field of capacitive position sensors in 2007 at the Department of Technologies in Electronics, Technical University of Kosice. His work is focused on interconnection techniques, fine thick film technologies, passive components and MEMS technologies.

Stanislav SLOSARCIK is a full professor at the Department of Technologies in Electronics, Technical University of Kosice. His work is focused on interconnection and mounting technologies in electronics, LTCC-based 3D-shaped modules, sensors and technologies of 3D integration of systems.

Peter BALOG defended his diploma thesis in 2014 at the Department of Technologies in Electronics, Technical University of Kosice where he defended his Ph.D. thesis in the same year. The theme of his dissertation thesis was "System for Movement of Paraplegics".